Lipid-derived nanoparticles for immunostimulatory RNA adjuvant delivery

Citation: Nguyen, D. N., K. P. Mahon, G. Chikh, P. Kim, H. Chung, A. P. Vicari, K. T. Love, et al. "Lipid-Derived Nanoparticles for Immunostimulatory RNA Adjuvant Delivery." Proceedings of the National Academy of Sciences 109, no. 14 (March 15, 2012): E797–E803.

As Published: http://dx.doi.org/10.1073/pnas.1121423109

Publisher: National Academy of Sciences (U.S.)

Persistent URL: http://hdl.handle.net/1721.1/91044

Version: Final published version: final published article, as it appeared in a journal, conference proceedings, or other formally published context

Lipid-derived nanoparticles for immunostimulatory RNA adjuvant delivery

David N. Nguyen[a,1], Kerry P. Mahon[b], Ghania Chikh[c], Phillip Kim[d], Hattie Chung[b], Alain P. Vicari[c], Kevin T. Love[b], Michael Goldberg[b], Steve Chen[b], Arthur M. Krieg[c], Jianzhu Chen[b], Robert Langer[a,b,d], and Daniel G. Anderson[a,b,d,2]

[a]Division of Health Sciences and Technology, Massachusetts Institute of Technology, Cambridge, MA 02142; [b]David H. Koch Institute for Integrative Cancer Research, Massachusetts Institute of Technology, Cambridge, MA 02142; [c]Pfizer Vaccines Research Ottawa, Pfizer Canada Inc., Ottawa, ON, Canada; and [d]Department of Chemical Engineering, Massachusetts Institute of Technology, Cambridge, MA 02142

Contributed by Robert Langer, January 4, 2012 (sent for review October 11, 2011)

The specific activation of Toll-like receptors (TLRs) has potential utility for a variety of therapeutic indications including antiviral immunotherapy and as vaccine adjuvants. TLR7 and TLR 8 may be activated by their native ligands, single-stranded RNA, or by small molecules of the imidazoquinoline family. However the use of TLR7/8 agonists for in vivo therapy is limited by instability, in the case of RNA, or systemic biodistribution and toxicity in the case of small molecule agonists. We hypothesized that unique lipid-like materials, termed "lipidoids," could be designed to efficiently deliver immunostimulatory RNA (isRNA) to TLR-expressing cells to drive innate and adaptive immune responses. A library of lipidoids was synthesized and screened for the ability to induce type I IFN activation in human peripheral blood mononuclear cells when combined with isRNA oligonucleotides. Effective lipidoid-isRNA nanoparticles, when tested in mice, stimulated strong IFN-α responses following subcutaneous injection, had robust antiviral activity that suppressed influenza virus replication, and enhanced antiovalbumin humoral and cell-mediated responses when used as a vaccine adjuvant. Further, we demonstrate that whereas all immunological activity was MyD88-dependent, certain materials were found to engage both TLR7-dependent and TLR7-independent activity in the mouse suggestive of cell-specific delivery. These lipidoid formulations, which are materials designed specifically for delivery of isRNA to Toll-like receptors, were superior to the commonly used *N*-[1-(2,3-dioleoyloxy)propyl]-*N,N,N*-trimethylammonium methylsulfate–RNA delivery system and may provide new tools for the manipulation of TLR responses in vitro and in vivo.

innate immunity | dendritic cell | drug delivery | high-throughput screening

The development of vaccine adjuvants has focused on innate immune activation, which is an important early aspect of the protective immune response (1–5). A first step in triggering innate immunity is the activation of pattern recognition receptors (PRRs) that allow for identification of pathogens without the need for prior education of an adaptive response. The Toll-like receptors (TLR) recognize conserved structures among a diverse group of pathogens (2). Nucleic acids can be recognized by TLRs 7, 8, and 9, which comprise a closely related subfamily whose expression differs by species and cell type, and whose function is compartmentalized to the endosome (2, 6, 7). RNA molecules that directly stimulate innate immune responses through mechanisms such as the TLR pathways have been functionally termed as immunostimulatory RNA (isRNA) (8). In humans, TLR7 is highly expressed and functional in plasmacytoid dendritic cells (PDCs) and B cells, whereas TLR8 expression is localized mostly to monocytes, myeloid dendritic cells (MDCs), and monocyte-derived dendritic cellss (moDCs) (9). The engagement of TLRs 7 and 8 results in a characteristic type I interferon response (e.g., IFN-α), promotion of an antiviral state with induction of IFN-stimulated genes, and suppression of viral replication (5, 10–13). TLR activation also leads to a coordinated Th1-biasing cytokine profile (1) that increases immune surveillance of cancer (7) and stimulates adaptive immunity by providing the necessary "danger signals" for efficient production of T-cell-mediated responses and class switching to high-affinity antibodies (1, 14).

Recent advances in characterizing and producing defined antigens has led to a plethora of vaccine targets, but protein vaccination alone lacks the immunostimulatory danger signals present in live attenuated or inactivated pathogen preparations (5, 15). By increasing coupling of innate and adaptive responses (4), introducing TLR stimulation as a vaccine adjuvant may be useful for improving immune responses to vaccines. However, clinical use of synthetic small molecule TLR7 and TLR8 agonists, such as imiquimod, in cancer and infectious disease (3, 5) has been restricted to topical application to avoid systemic distribution, exuberant activation of innate immune responses (3, 16), and off-target activity (17). Targeted delivery of nucleic acid agonists may allow for localized activation of specific cells without the side effects of systemic small molecule agonists. Utilization of unprotected small single-stranded RNAs (ssRNAs), the natural ligands for TLR7/8 (6, 18), is impractical due to low stability, nuclease degradation (19–21), and the requirement of endosomal uptake for induction of TLR7/8 responses (11, 18, 22). Drug delivery systems have been shown to enhance both the efficiency and immunostimulatory side effects of siRNAs (23–26) yet to our knowledge no systems designed specifically for delivery of isRNAs to TLRs have been reported.

We hypothesized that controlled delivery of isRNA to TLR7 or TLR8 with synthetic nanoparticles could mimic the robust immune responses triggered by viral infection through efficient and localized activation of innate immune responses. Here we develop lipid-like materials, termed "lipidoids" (27), specifically capable of inducing robust isRNA-mediated TLR stimulation. We detail how lipidoid-isRNA nanoparticles can be synthesized, screened, and formulated to enhance humoral and cell-mediated immunity. Further, we discuss evidence supporting a mechanism of cell-specific targeting and MyD88-dependent activation of TLRs by lipioid-isRNA nanopartcles in vitro and in vivo.

Results

In Vitro Screening of Lipidoids Capable of isRNA Delivery. A preliminary library of lipidoid molecules was generated by combinatorial addition of alkyl-acrylate or alkyl-acrylamide tails to primary or

Author contributions: D.N.N., K.P.M., G.C., P.K., H.C., A.P.V., S.C., A.M.K., J.C., R.L., and D.G.A. designed research; D.N.N., K.P.M., G.C., P.K., H.C., A.P.V., K.T.L., and S.C. performed research; K.P.M., K.T.L., and M.G. contributed new reagents/analytic tools; D.N.N., G.C., P.K., H.C., A.P.V., and D.G.A. analyzed data; and D.N.N., K.P.M., G.C., R.L., and D.G.A. wrote the paper.

The authors declare no conflict of interest.

[1]To whom correspondence may be addressed at: Massachusetts Institute of Technology, Building 76, Room 653, 500 Main Street, Cambridge, Massachusetts 02142. E-mail: dgander@mit.edu.

[2]Present address: Stanford University School of Medicine, Stanford, CA 94305

See Author Summary on page 5150 (volume 109, number 14).

This article contains supporting information online at www.pnas.org/lookup/suppl/doi:10.1073/pnas.1121423109/-/DCSupplemental.

secondary amine-containing cores (Fig. S1*A*) following a simple solvent-free synthesis (Fig. S1 *B* and *C*). Lipidoid compounds are named according to the tail composition (designated by two letters) followed by number of tails if purified (in parentheses) and then by the amine core (designated by number) as described in Fig. S1. The 96 different lipidoid synthesis reactions (Table S1) included a variety of carbon alkyl tail lengths and amine-core structures. Lipidoid–RNA complexes were formed at four different mass ratios of lipidoid to RNA (15, 10, 5, 2.5 to 1) and screened in vitro for delivery in human peripheral blood mononuclear cells (PBMCs) using a high-throughput cell-based assay that detects type I IFN (28). The short single-stranded guanine-uracil (GU)-rich R-006 isRNA oligonucleotide has been shown to be an active TLR7 and TLR8 agonist inducing production of IFN-α and Th1-type cytokines across multiple species including human and mouse (29). To control for direct lipidoid-mediated immunostimulatory activity or toxicity, we also performed negative screening against the control R-1263 sequence ssRNA oligonucleotide, which has similar structure to R-006 but exhibits low TLR7 and TLR8 activity (29).

Many of the lipidoid–RNA complexes tested exhibited some level of immunostimulatory activity (Fig. 1 and Fig. S2). Almost 900 different conditions were tested that included different lipidoids with isRNA or control RNA at various lipidoid/RNA ratios. Of these, 106 conditions generated activity greater than half that of lipofectamine (L2K), which was used to normalize activity across donor PBMC batches. Although too toxic for in vivo administration, L2K has proven to be an effective transfection agent in vitro and a useful delivery screening benchmark (27). Excluding lipidoid formulations that were immunostimulatory with both the R-006 and R-1263 sequences, 14 distinct lipidoid materials were found to have activity equal to or greater than that of L2K combined with R-006. The 100-core diamine (Fig. S1*A*) was highly represented in this active subset. Of the seven 100-core lipidoid products tested, five enabled efficient delivery of R-006 including the top three lipidoid compounds at any weight ratio (Fig. 1, Fig. S2, and Fig. S3*A*).

Second-Generation Lipidoids Based on the 100-core. The 100-core has two primary amines that each can be substituted with up to two alkyl tails each for a total of four possible substitutions. A second-generation set of 100-core lipidoids incorporating short chain lengths and mixed alkyl chains was synthesized and evaluated for potential to deliver isRNA. We focused on three- and four-tail versions of the 100-core based on prior work indicating that fully (n) and partially (n-1)-substituted lipidoids exhibit the most efficient siRNA delivery (27). These 100-core lipidoids were synthesized by stepwise substitution of each primary amine (Fig. S1*D*) with a mixture of ND and NA tails, further identified as lipidoid "I" (I-3, three tails, and I-4, four-tails), or a mixture of ND and LD tails, further identified as lipidoid "II" (Fig. 2). Purified lipidoids I-3 and II-3 were soluble in sodium acetate whereas lipidoids I-4 and II-4 were insoluble in aqueous solutions. Upon repeat screening in vitro, lipidoids I and II exhibited high levels of isRNA delivery that were RNA specific and greater than that of ND(5)-98-1 (Fig. S3*B*), a lipidoid material previously shown to have high capacity for siRNA delivery in vitro and in vivo (27). Thus, the 100-core and second-generation derivatives were further investigated for in vivo isRNA delivery.

In Vivo Optimization of Lipidoid–RNA Nanoparticles. Previous work has demonstrated that formulation parameters and lipidoid: RNA (L/R) ratio can affect in vivo performance of lipidoid nanoparticles (23, 26, 30). To increase solubility and stability, lipidoids at 10:1, 11.5:1, or 15:1 L/R ratio were formulated with poly(ethylene-glycol) (PEG) and cholesterol (Ch) and extruded through 80 nm pores to generate nanoparticles. The particles were then either lyophilized or dialyzed to remove ethanol. Lyophilized nanoparticles under the conditions tested were found to have a heterogeneous size distribution into the micron range and aggregated after resuspension in HBSS (Table S2). Dialyzed nanoparticles remained stable in size below 200 nm for up to 1 mo (Table S3).

Nanoparticles of multiple different lipidoids encapsulating R-006 RNA were screened by s.c. injection in BALB/c mice, and the time course of IFN-α, interferon gamma-induced protein 10 (IP-10), and IL-6 induction was monitored over 24 h (Fig. S4 *A* and *B*). These cytokines were selected as markers of PDC (IFN-α and IP-10) and MDC (IL-6) activation (31, 32) and have been previously observed in response to R-006 RNA (29). *N*-[1-(2,3-dioleoyloxy)propyl]-*N,N,N*-trimethylammonium methylsulfate (DOTAP) has previously been used to facilitate cellular uptake and to investigate isRNA effects in vivo (18, 21). Lipidoids I-4 and II-4 consistently outperformed DOTAP and ND(5)-98-1. In direct comparisons, the dialyzed formulations of second-generation 100-core lipidoids I-4 and II-4 at a 15:1 L/R ratio had the highest propensity for cytokine induction (Fig. 3). Furthermore, T, B, and NK cells were all activated in response to both I-4 and II-4 lipidoid nanoparticles (Fig. S4*C*). Both I-4 and II-4 nanoparticles exhibited dose-dependent immunostimulation following s.c. administration (Fig. S4*D*). Thus, dialyzed lipidoid–RNA nanoparticles (LRNP) of lipidoids I-4 and II-4 at an L/R ratio of 15:1 were used for all subsequent in vivo investigations.

Increased Innate and Adaptive Immune Responses. We investigated clinically relevant endpoints in two mouse models of innate immune activation addressing antiviral and vaccine adjuvant properties. Because LRNP-II induced the greater amount of IFN-α secretion, these nanoparticles were tested in an established in vivo model of influenza infection previously shown to be sensitive to isRNA-triggered interferon and cytokine responses (23). LRNP-II were formulated with R-006, R-1263, or without RNA,

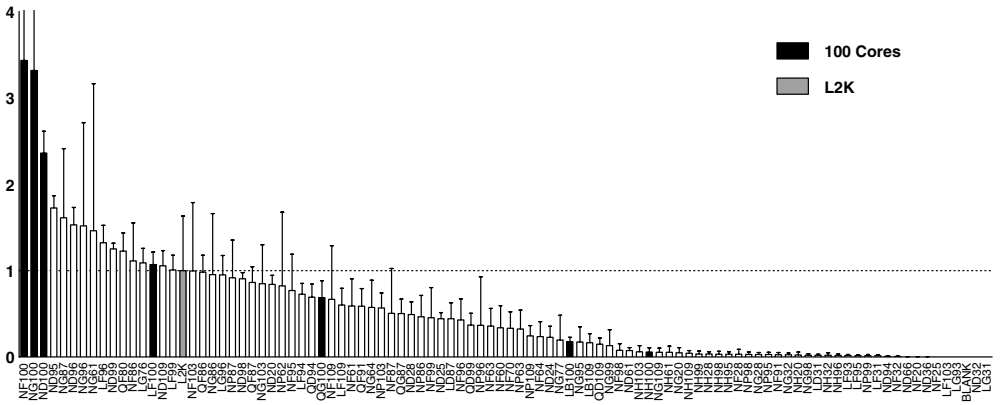

Fig. 1. Initial screening of lipidoid library for isRNA delivery. The highest relative type I IFN activity per unique compound, with either active or control RNA at any weight ratio, is shown for 96 lipidoids. All lipidoids were screened for isRNA delivery to human PBMCs in vitro independently with 200 μg of either immunostimulatory R-006 or control R-1263 comprising over 900 unique transfection experiments. Type I interferon activity was normalized for each batch of PBMCs to activity of L2K complexed with R-006 (gray bar, dotted line). 100-core lipidoids highlighted by solid black bars. Error bars represent standard deviation, $n = 4$.

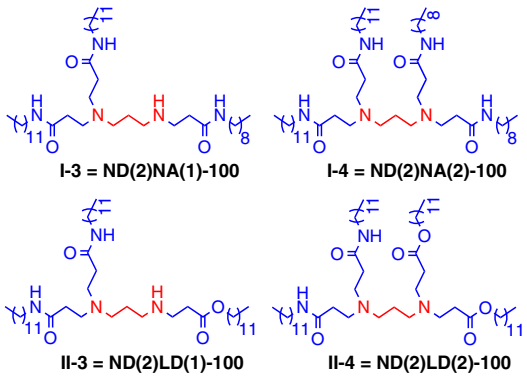

Fig. 2. Structures of second-generation lipidoids based on 100 core. Second-generation lipidoids were designed based on the 100 core (red). An ND(2)-100 precursor was substituted with the 10-carbon alkyl-acrylamide NA (lipidoid I) or the 12-carbon alkyl-acrylate LD (lipidoid II) and purified into single isomer components with either three or four total tails.

and injected s.c. into 129sv mice. After 9 h, mice were challenged intranasally with a supralethal dose (12,000 pfu) of influenza A/PR8 virus. Lung titers were measured 24 h postchallenge and found to be reduced 10-fold by isRNA delivery (Fig. 4*A*) relative to untreated control. Further, this antiviral prophylaxis was only observed for the immunostimulatory R-006 RNA, whereas neither control R-1263 nanoparticles nor empty nanoparticles without RNA (II-4 + Blank) resulted in significant reduction of viral titer.

We further investigated the potential of both LRNP-I and LRNP-II as adjuvants of vaccination with the model protein antigen chicken ovalbumin (Ova). C57Bl/6 mice were vaccinated by i.m. injections with Ova protein mixed with comparison adjuvants represented by LRNPs, DOTAP–RNA complexes, or CpG oligodeoxynucleotide (ODN) 1826, which is a mouse-specific B-class TLR9 agonist previously shown to adjuvant Ova antigen responses (33); two different pan-species B-class CpG ODN have shown enhancement of antibody titers against various antigens in clinical trials (5, 34, 35) and one is now in phase 3 testing in a hepatitis B vaccine (Heplisav, Dynavax). Immunization with LRNPs increased the magnitude of Ova-specific IgG by 3 to 4 log orders compared to immunization with protein alone (Fig. 4*B*). A significant increase in total IgG was observed for LRNP-I with both R-006 and R-1263, but for LRNP-II only immunization with R-006 RNA resulted in statistically greater levels of IgG antibody. Vaccination with either LRNP resulted in an increase in both IgG1 and IgG2c subclasses compared to protein alone (Fig. S5*A*). The increase in Th1-biased IgG2c subclass was notable compared to immunization with Ova protein alone although not as striking as it was for Ova mixed with CpG-ODNs, which have previously been shown to induce a strong Th1 bias (36, 37). LRNP adjuvants also increased absolute IgG2c titers, but preserved the Th2-associated IgG1 bias of protein vaccination alone.

More strikingly, LRNP also greatly enhanced cell-mediated immune responses to Ova. Both LRNP-I+R-006 and LRNP-II +R-006 induced greater numbers of splenic Ova-antigen-specific $CD8^+$ T cells than either CpG ODN 1826 or DOTAP+R-006 complexes, and all LRNP formulations increased antigen-specific $CD8^+$ T cells to levels greater than that with Ova vaccination alone (Fig. 4*C*). Using CpG ODN on its own as used here may be suboptimal for adjuvant effect as greater immunogenicity has been demonstrated in mice when CpG ODN is combined with an additional adjuvant possessing delivery properties (34, 37, 38). At low dose (10 μg) of LRNP-II nanoparticles, the increase in percentage of reactive CD8+ positive T cells was significantly greater with the R-006 RNA than R-1263. However, for LRNP-I the percentage of reactive CD8+ positive T cells was large but not significantly different between active R-006 and control R-1263 RNA. In vitro restimulation of splenocytes from vaccinated animals resulted in large increases in the Ova-specific secretion of the Th1-biasing cytokines IFN-γ and IL-2 (Fig. S5*B*). Increases of the Th2-associated cytokines IL-10 and IL-4 were also observed.

Characterization of Innate Immune Activation. LRNP-II exhibited 10-fold greater IFN-α and IP-10 responses than LRNP-I nanoparticles, which potently activated IL-6 following s.c. injection (Fig. S4*D*). We hypothesized that the lipidoid-specific cytokine profiles observed were due to preferential uptake and activation of different cell types following s.c. administration. We compared delivery of isRNA to primary monocytes or PDCs isolated from human PBMCs using lipidoids I-3 and II-3, the three-tailed versions of I and II that had greater isRNA activity in vitro (Fig. S3*B*). Lipidoid I-3 complexed with R-006 induced type I interferons from isolated CD14+ cells (i.e., monocytes), but not from isolated PDCs (Fig. S6*B*). Conversely, lipidoid II-3 complexed with R-006 induced large amounts of type I interferon production in PDCs but considerably less from CD14+ cells (monocytes).

After i.v. injection in the 129sv strain of mouse, LRNPs activated more robust responses than the s.c. route, and isRNA specificity was observed in stimulation of serum IFN-α and IP-10 with almost no activity of the control R-1263 RNA (Fig. S6*A*). However, LRNP formulated with R-1263 did induce IL-6 when injected i.v. raising concerns for increased nonspecific activation with i.v. injection, and this observation was most pronounced at the earliest time points with LRNP-I. We thus further investigated directly the role of TLRs in differential recognition of LRNPs.

The TLRs utilizing the common MyD88 pathway are TLR1, TLR2, TLR5, TLR6, TLR7, TLR8, and TLR9 (11). Because knock-out mice for all the TLRs were not readily available, we investigated TLR-specificity of LRNP-I in vitro in a human cell line stably expressing human TLRs. HEK293 cell lines stably expressing human TLRs 2, 3, 4, 5 or 6 were incubated with LRNP + R-006 without observation of any TLR-mediated activity above background (Fig. S6*C*). HEK293 cells stably transfected with TLR8, and TLR7 to a lesser extent, exhibited dose-dependent activation by LRNP-I incorporating R-006 RNA (Fig. S6*D*).

LRNP were also investigated in knock-out mouse models of the MyD88, TLR4, TLR7, and TLR9 genes and compared to wild-type (WT) controls on matched backgrounds (Fig. 5). Production of IFN-α, IP-10, and IL-6 were all dependent on MyD88 signaling for both LRNP-I and LRNP-II. However, only IFN-α and IP-10 production were also dependent upon TLR7. In the C57BL/6 strain, we observed that IL-6 production in response to LRNP-II was RNA specific and completely dependent upon TLR7. However, IL-6 activation in the same strain by LRNP-I appears to be only partially TLR7-dependent at a 50 μg RNA

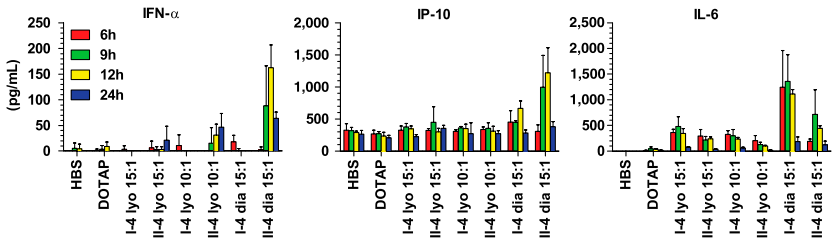

Fig. 3. In vivo screening for activation of innate immune responses following injection of formulated lipidoid–RNA nanoparticles. Lipidoid–RNA nanoparticles formulated with 100 ug R-006 RNA were injected s.c. in BALB/c mice ($n = 3$ or 4). R-006 formulated with DOTAP and a mock injection with HBSS were included as controls. Blood was collected at 6, 9, 12, and 24 h following injection and indicated cytokines were measured by ELISA.

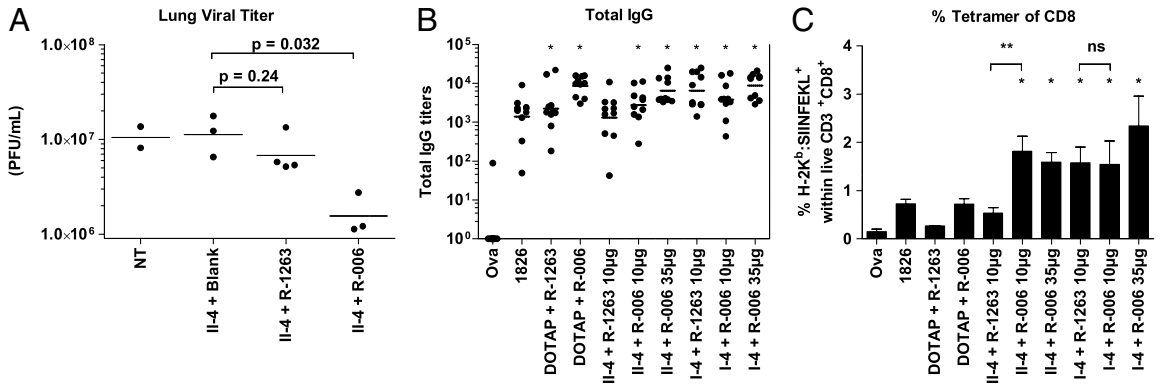

Fig. 4. In vivo adjuvant activity of formulated lipidoid–RNA nanoparticles (*A*) Prophylaxis against influenza infection. Lipidoid II-4 was formulated with R-006 RNA, R-1263 RNA, or without RNA (II-4 + blank) as a control and 50 μg RNA basis was injected s.c. in 129Sv mice. Lung viral titer was measured 24 h after challenge with 12,000 pfu of influenza (PR8) virus. Individual titers shown with geometric mean for each group represented by a bar. *p* values indicated for two-way *t*-test. (*B*–*C*) Adjuvant activity in chicken ovalbumin protein vaccination of C57Bl/6 mice together with lipidoid I-4 or lipidoid II-4 nanoparticles. Vaccination was also done with DOTAP-formulated RNA, CpG ODN 1826 (TLR9 agonist), or without adjuvant. Immunization was performed i.m. on days 0, 14, and 21, and samples were collected at day 28. (*B*) Total serum Ova-specific IgG. Individual titers shown with geometric mean for each group represented by a bar. (*C*) Spleen CD8$^+$ T cells specific for the SIINFEKL peptide fragment of the Ova protein. * $p = 0.05$ by one-way ANOVA with Dunn's Multiple Comparison posttest for means with unequal variance compared to Ova group ** $p = 0.05$ by one-way ANOVA with Dunn's Multiple Comparison posttest.

dose i.v. Further, IL-6 activity was completely abolished regardless of RNA without MyD88 signaling (Fig. 5). Incomplete reduction in IL-6 for LRNP-I + R-006 nanoparticles was observed in TLR − /− mice, and no inhibition was observed for LRNP-I + R-1263 nanoparticles. TLR4 and TLR9 were not required for cytokine production for either LRNP with either RNA, indicating that neither LPS nor immunostimulatory DNA contamination was responsible for IL-6 induction.

Given the differences in vaccine responses observed for LRNP-I compared to LRNP-II, we further investigated LRNP-I adjuvant properties in mice deficient in MyD88. Antigen-specific responses following immunization revealed a marked dependence upon MyD88 for increasing both cell-mediated and humoral immunity. Compared to wild-type controls, the humoral response of MyD88$^{-/-}$ mice exhibited reduced generation of total IgG titer for CpG ODN, lipidoid nanoparticles, and DOTAP–RNA complexes but not Ova antigen alone or polyI:C (Fig. S7*A*). MyD88$^{-/-}$ mice also exhibited complete loss of class switching to IgG2c (Fig. S7*B*) except for polyI:C. Additionally, a diminished cell-mediated response in MyD88$^{-/-}$ mice was observed with reduced antigen-specific cytotoxic T lymphocyte activity (Fig. S7*C*) and overall decreased numbers of antigen-specific T cells (Fig. S7*D*).

Discussion

Many groups have focused on strategies to chemically or physically alter nucleic acids such as siRNAs (25, 26, 39–41) to increase serum stability or render them immuno-silent; however, to our knowledge the development of delivery systems to intentionally enhance isRNA activity has not been reported. Here we develop a library of lipidoid materials for delivery of isRNA. These materials were able to condense isRNA molecules into nanoparticles and deliver isRNA molecules into endosomes of immune cells where they could trigger TLR-mediated responses. The RNA delivery systems reported herein have been specifically designed to incorporate these functionalities for the purpose of isRNA delivery.

Analysis of the chemical structures of lipidoids most efficient for isRNA delivery revealed that the isRNA delivery functionality was correlated with certain amine-core structures. Materials based upon the same cores (e.g., 100, 86, 87) exhibited similar properties (Fig. 1 and Fig. S2). It has been previously theorized that charge interaction is responsible for the nucleic acid packaging, release, and the endosomal escape properties of polyamines and positively charged lipids (25, 42). Following particle uptake, we hypothesize that the chemical properties of the available amines influence the intracellular location of release of the isRNA in such a manner that the isRNA payload remains within the endosome. Materials highly efficient for DNA delivery and RNA interference likely facilitate endosomal escape and thus may be poor agents for delivery of isRNA to TLRs in the endosome. Consistent with this hypothesis, lipioids previously found useful for delivery of double-stranded small interfering RNAs (27) (e.g., ND(5)-98-1) were not as useful for delivery of isRNA. Structures based upon the diamine core 100 were the most efficient in isRNA delivery across a variety of tail lengths. Additionally, lipidoids based upon the structurally and chemically similar 86 and 87 cores were highly immunostimulatory even with control RNA (Fig. S2*A*) possibly due to toxicity or direct TLR interaction.

Whereas the core material appears to be the major determinant of isRNA activity, it is clear that the alkane tails also influence delivery properties of the formulated nanoparticle (Fig. S3*A*) including cell-specific targeting. Tail chemistry can also influence the ability of a lipid to destabilize a cellular or endosomal membrane thus modifying rate of endosomal retention and release (25, 30). Further, our experience with lipidoids has shown that different tail-lengths or mixtures can result in unexpectedly enhanced functionality (43, 44). Thus, by screening and iteration based upon these design principles, we were able to explore a large chemical/functional space resulting in two novel 100-core lipidoids with mixed tails (I and II) highly efficient for isRNA delivery (Fig. 3, Fig. S4).

Although they both contain the same 100-amine core, lipidoids I and II exhibited differential patterns of innate immune activation suggestive of delivery to different cell types or different signaling pathways. The type I IFN and IP-10 production pattern associated with LRNP-II may be indicative of delivery of R-006 to TLR7 in PDCs. In humans and mice IFN-α is mostly produced by PDCs in responses to ssRNA activation of TLR7 although MDCs and monocyte-lineage cells can also secrete IFN-α with less potency (9, 45). IP-10 (CXCL10) is also produced primarily by PDCs through TLR7 in a ssRNA-dependent manner (6, 18, 32). However, IL-6 is primarily produced by MDCs, monocytes, and moDCs upon stimulation (9), though it can also be produced by murine PDCs in response to viral ssRNA (6, 18). Thus the activity of lipidoid I in terms of high IL-6 production is consistent with isRNA delivery preferentially to moDCs or MDCs. This hypothesis is further supported by the observation of cell-type-specific isRNA-mediated activation in vitro in human peripheral blood PDCs and monocytes (Fig. S6*B*).

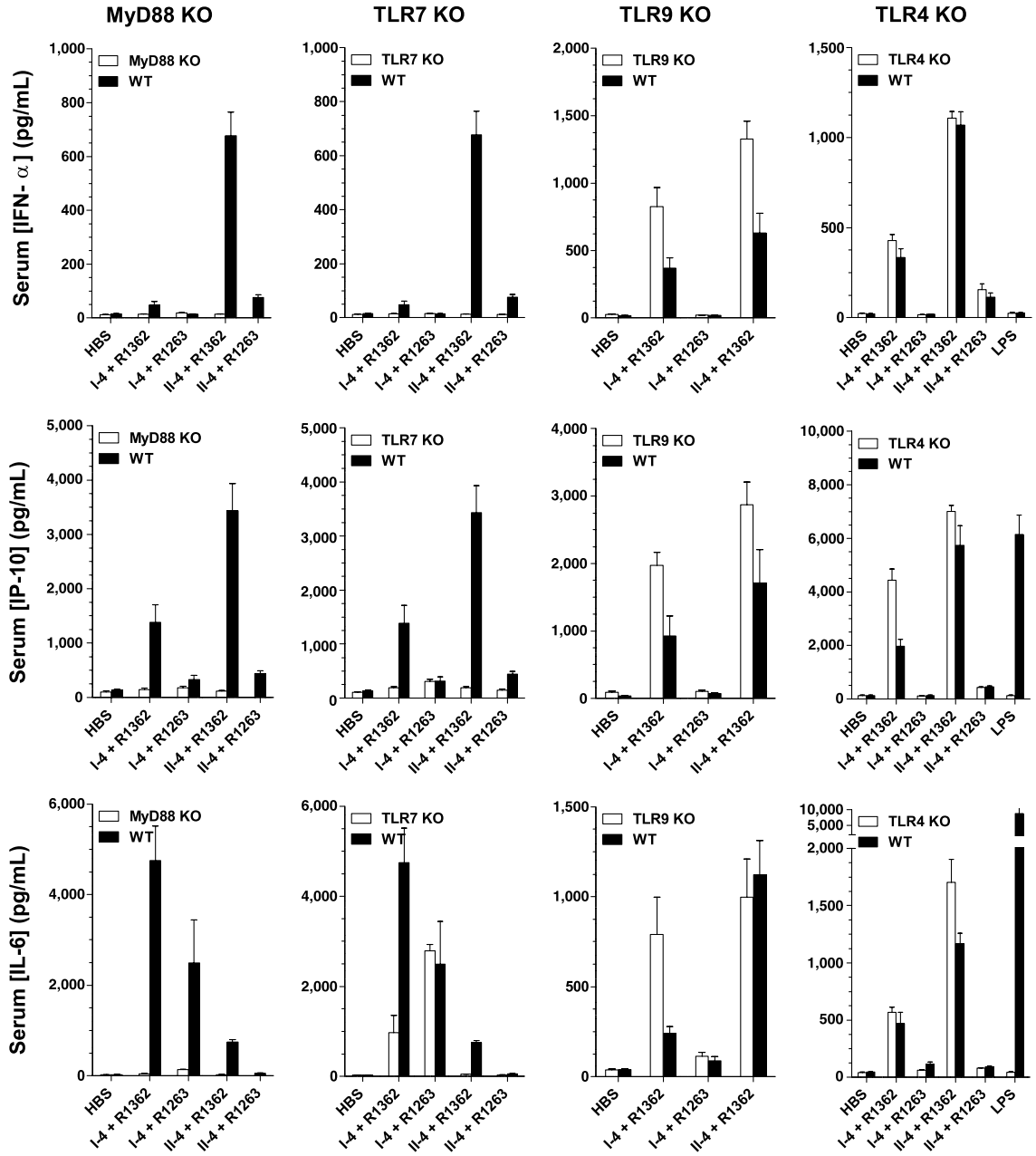

Fig. 5. Characterization of cytokine response from lipidoid–RNA nanoparticles in vivo. Lipidoids I-4 and II-4 were formulated with the strong TLR7/8 agonist R-006 RNA and the weak TLR7/8 agonist R-1263 RNA as control. Serum cytokine response of IFN-α (*Top*), IP-10 (*Middle*), and IL-6 (*Bottom*) at 6 h compared to strain background-matched controls following i.v. injection of 50 μg RNA into MyD88$^{-/-}$ or TLR7$^{-/-}$ mice, or 30 μg RNA into TLR9$^{-/-}$ or TLR4$^{-/-}$ mice; LPS = lipopolysaccharide; (n = 3 or 4).

The LRNP may activate more than one TLR. In the mouse, cell-specific segregation of TLR7 is less distinct than it is in humans (8, 11, 18); TLR7 is well-expressed in mouse MDCs and moDCs. Both IFN-α and IP-10 production were clearly TLR7- and MyD88-dependent in mice (Fig. 5) confirming an isRNA-specific TLR7-mediated mechanism. Recently it has been shown that mouse TLR8, previously thought to be nonfunctional (6, 18, 19, 46), can be activated under certain conditions (29, 47, 48). We hypothesize that TLR8 may play a partial role in LRNP-I isRNA-mediated activation of IL-6. In support of this hypothesis both TLR7 and TLR8 showed clear activity in response to LRNP-I stimulation in a human cell culture TLR-overexpression model (Fig. S6*D*) whereas the remaining MyD88-dependent TLRs were not stimulated (Fig. S6*C*). The IL-6 production induced by lipidoid-mediated isRNA delivery in TLR7-deficienct mice but not MyD88-deficient mice (Fig. 5) also indicates a possible role for isRNA stimulation of another MyD88-dependent receptor although no TLR8$^{-/-}$ mouse model was available to directly test the role of TLR8 responses to LRNPs in vivo. Together these data indicate roles for TLR7 and another MyD88-dependent function, possibly TLR8, for the induction of IL-6 by LRNP-I.

Prophylactic administration of LRNP-I resulted in suppression of influenza virus replication in the mouse lung (Fig. 4*A*) specific to the immunostimulatory activity of R-006 RNA. These data indicate that s.c. injections of lipidoid-encapsulated isRNA can achieve sufficient systemic innate immune stimulation to combat viral infection. Because they activate the same receptors as viruses resulting in a variety of cytokines and interferons, lipidoid isRNA delivery may resemble the innate response to infection by RNA viruses. Imiquimod, a TLR7/8 agonist, has seen extensive

clinical use (3, 5) as a topical chemotherapeutic and antiviral. Experimental therapies employing TLR7 agonists have also demonstrated some clinical benefit in viral hepatitis (49), however, adverse immunologic events related to widespread biodistribution were observed at therapeutic doses (50, 51) including unacceptable toxicity in a human trial of oral imiquimod (52). No adverse effects were observed in mice injected with LRNPs in this study, though long-term and dose-response effects of LRNP administration need to be investigated. A restricted delivery approach such as LRNPs may limit the systemic distribution by localizing initiation of immune responses to the application site and draining lymph nodes as well as targeting uptake to specific cell types. Thus the endogenous antiviral-like response activated by LRNPs may be an attractive alternative therapy for conditions currently treated with recombinant IFN-α regimens.

The development of vaccine adjuvants that increase both humoral and cell-mediated immune responses by targeting TLRs represents a promising approach for the field of vaccine development (3, 5, 10). A hallmark of this cellular immunity is expansion of antigen-specific $CD8^+$ T cells, which was increased by immunization with either LRNP-I or LRNP-II (Fig. 4*C*). LRNP adjuvants increased secretion of Th1-biasing cytokines upon restimulation (Fig. S5*B*), which are associated with control of intracellular pathogens (2) and cancers (7). Efficient T-cell activation with multifunctional quality can lead to memory responses that confer protective immunity for long periods of time (1, 14, 53). Further studies will be necessary to evaluate the memory function and quality of T-cell responses to protein vaccines adjuvanted by LRNPs.

Class switching and production of IgG2c in B-cells and efficient antigen-specific T-cell induction requires activation of MyD88 (54). If the adjuvant mechanism of LRNP-I was completely due to activation of TLR-dependent innate immune responses, then these responses would be expected to be dependent upon MyD88. However, comparison of vaccine responses in wild-type and MyD88-deficient mice showed that although loss of MyD88 markedly reduced both cell-mediated and humoral immune responses, some adjuvant activity was maintained particularly with respect to generation of (non-IgG2c) IgG antibodies (Fig. S7*B*) indicating an additional role of a non-MyD88-dependent adjuvant effect. Commonly used adjuvants including alum, Freund's adjuvant, and squalene increase immune responses by both enhancing innate immune responses (4) and sustaining antigen availability and presentation in draining lymph nodes (55). Thus, in addition to providing isRNA-mediated innate signals, lipidoid nanoparticles may also enhance the delivery of protein antigens or TLR agonists to tissue-resident and lymphatic dendritic cells (55) thereby increasing vaccine responses.

In conclusion, combinatorial chemistry and high-throughput screening methods have enabled development of libraries of materials for isRNA delivery that provide for specific activation of immune responses. We report the development of unique delivery systems specifically designed to deliver isRNA in the context of a vaccine adjuvant or for use in immune prophylaxis against viral infection. Here we have directly shown LRNPs to be more efficient for isRNA delivery than currently available agents such as lipofectamine, DOTAP, or even the previously reported lipidoid ND(5)-98-1 (23, 27). Immunostimulatory RNA delivery to PDCs using formulations such as LRNP-II may be useful for antiviral applications, whereas delivery using LRNP-I may be most useful for activating monocytes and MDCs to enhance vaccine responses. Our screening revealed two promising candidate materials for future development, and further refinement of lipidoid design and nanoparticle formulation techniques may lead to even more specific and robust effects. Further development of such vehicles for controlled TLR7 and 8 stimulation, including additional optimization and safety assessment in larger animals, may have future clinical utility.

Materials and Methods

A summary of experimental techniques is presented here. For full details and methods, please see the *SI Materials and Methods*.

Lipidoid Synthesis and High-Throughput Screening for isRNA Delivery. Lipidoids were synthesized in a combinatorial fashion as depicted in Fig. S1 as previously described (27) by reacting primary and secondary amine-containing cores with alkyl-acrylate or alkyl-acrylamide tails. A complete list of crude lipidoids screened is found in Table S1. Second-generation lipidoids based on the 100-core diamine were synthesized in a four-step process (Fig. S1*D*) and renamed lipidoids I and II for clarification. Lipidoid products were complexed with RNA in sodium acetate at 15, 10, 5, and 2.5 : 1 mass ratios of lipid to RNA. RNAs R-006 or R-1263 were fully phosphorothioate-modified, 20-base, ssRNA synthesized by Coley Pharmaceuticals with sequences as previously described (29). PBMCs were isolated from donor-blind buffy-coat packs obtained from the Massachusetts General Hospital blood bank. Complexes were added to PBMCs, plated at 5×10^5 cells/well, for a final RNA concentration of 200 ng RNA per well (1 μg/mL, approximately 140 nM). Additionally, PBMCs were incubated with R-006 and L2K, according to manufacturers siRNA transfection protocols, to control for donor PBMC variability in maximum type I IFN secretion capacity. After 16–20 h of incubation, PBMC supernatants were stored at −80 °C for later quantification of type I interferon activity using a high-throughput cell-based detection assay as previously described (28).

Formulation and Characterization of Lipidoid–RNA Nanoparticles. Purified lipidoid was codissolved in ethanol with cholesterol and C16 mPEG 2000 ceramide at a 15:0.8:7 mass ratio (L:C:P) in a mixture of ethanol and sodium acetate. Lipidoid/Ch/PEG were added to RNA at a 15, 11.5, or 10:1 mass ratio (L:R). Lipidoid–RNA nanoparticles were then extruded through a double 200 nm membrane and then twice through a double 80 nm membrane (Whatman) on a Northern Lipids extrusion system at 40 °C. Prior to injection, nanoparticles were either dialyzed at 3,500 molecular weight cutoff in HBSS or lyophilized with 10 mg/mL sucrose. Final RNA concentration was determined by modified Ribogreen (Invitrogen) assay. No bacterial endotoxin was detected by limulus amebocyte lysate assay (Lonza) in any batches of nanoparticles.

In Vivo Characterization of Innate Immune Responses. All animal studies, except for influenza prophylaxis studies, were conducted at Coley Pharmaceuticals (now Pfizer Canada) under the approval of the institutional care committees and in accordance with the guidelines set forth by the Canadian Council on Animal Care. Mouse studies of influenza prophylaxis were conducted at the Massachusetts Institute of Technology (Cambridge, MA), where animals were cared for according to the guidance of the Division of Comparative Medicine. Animals were monitored for the duration of all experiments for adverse behavior or decrease in normal activity that might indicate toxicity or adverse inflammatory responses. Lipidoid–RNA nanoparticles were formulated with either R-006 or R-1263 RNA at 15:1 ratio (lipidoid to RNA), dialyzed to remove ethanol, and diluted in HBSS prior to injection under isofluorane anesthesia. Lipidoid nanoparticles were injected s.c. or by i.v. tail vein injection in 129Sv mice at indicated doses. Serum samples were analyzed for levels of IFN-α and cytokines at indicated time points. TLR-mediated responses were investigated following i.v. injection in TLR-deficient or genetic-background-matched WT controls. Prophylaxis of influenza infection models was conducted as previously described (23). Briefly, lipidoid–RNA nanoparticles were injected s.c. at 50 μg RNA per mouse. After 9 h, mice were infected by intranasal instillation with 12,000 pfu influenza A virus A/PR/8/34 (PR8). Lungs viral titer was quantified at 24 h after infection. Adjuvant studies of lipidoid I and II isRNA nanoparticles were performed by mixing indicated doses of lipidoid-formulated RNA with 20 μg chicken Ova immediately prior to i.m. injection into C57Bl/6 mice or $MyD88^{-/-}$ on the C57Bl/6 background. Mice were dosed at days 0, 14, and 21, then blood and splenocytes were collected at day 28. Plasma anti-Ova total IgG, IgG1, and IgG2c were determined by sandwich ELISA. Splenocytes were assessed using a chromium release assay for cytotoxic T cells and flow-cytometry-based tetramer analysis for quantifying antigen-specific T cells as previously described (56).

ACKNOWLEDGMENTS. This work was supported in part by grants from the National Institutes of Health EB00244 (to R.L. and D.G.A.) and AI56267 (to J.C.) and from the National Institute of Allergy and Infectious Diseases Contract HHSSN266200400044C (to G.C. and A.M.K.).

1. Iwasaki A, Medzhitov R (2004) Toll-like receptor control of the adaptive immune responses. *Nat Immunol* 5:987–995.
2. Zhang SY, et al. (2007) Human Toll-like receptor-dependent induction of interferons in protective immunity to viruses. *Immunol Rev* 220:225–236.
3. Meyer T, Stockfleth E (2008) Clinical investigations of Toll-like receptor agonists. *Expert Opin Investig Drugs* 17:1051–1065.
4. Pashine A, Valiante NM, Ulmer JB (2005) Targeting the innate immune response with improved vaccine adjuvants. *Nat Med* 11(Suppl 4):S63–68.
5. Kanzler H, Barrat FJ, Hessel EM, Coffman RL (2007) Therapeutic targeting of innate immunity with Toll-like receptor agonists and antagonists. *Nat Med* 13:552–559.
6. Heil F, et al. (2004) Species-specific recognition of single-stranded RNA via toll-like receptor 7 and 8. *Science* 303:1526–1529.
7. Schon MP, Schon M (2008) TLR7 and TLR8 as targets in cancer therapy. *Oncogene* 27:190–199.
8. Hornung V, et al. (2005) Sequence-specific potent induction of IFN-alpha by short interfering RNA in plasmacytoid dendritic cells through TLR7. *Nat Med* 11:263–270.
9. Jarrossay D, Napolitani G, Colonna M, Sallusto F, Lanzavecchia A (2001) Specialization and complementarity in microbial molecule recognition by human myeloid and plasmacytoid dendritic cells. *Eur J Immunol* 31:3388–3393.
10. Borden EC, et al. (2007) Interferons at age 50: Past, current and future impact on biomedicine. *Nat Rev Drug Discov* 6:975–990.
11. Akira S, Takeda K (2004) Functions of toll-like receptors: Lessons from KO mice. *C R Biol* 327:581–589.
12. Cristofaro P, Opal SM (2006) Role of Toll-like receptors in infection and immunity: Clinical implications. *Drugs* 66:15–29.
13. Honda K, Taniguchi T (2006) IRFs: Master regulators of signalling by Toll-like receptors and cytosolic pattern-recognition receptors. *Nat Rev Immunol* 6:644–658.
14. Steinman RM, Banchereau J (2007) Taking dendritic cells into medicine. *Nature* 449:419–426.
15. Delgado MF, et al. (2009) Lack of antibody affinity maturation due to poor Toll-like receptor stimulation leads to enhanced respiratory syncytial virus disease. *Nat Med* 15:34–41.
16. Marshak-Rothstein A (2006) Toll-like receptors in systemic autoimmune disease. *Nat Rev Immunol* 6:823–835.
17. Romagne F (2007) Current and future drugs targeting one class of innate immunity receptors: The Toll-like receptors. *Drug Discov Today* 12:80–87.
18. Diebold SS, Kaisho T, Hemmi H, Akira S, Reis e Sousa C (2004) Innate antiviral responses by means of TLR7-mediated recognition of single-stranded RNA. *Science* 303:1529–1531.
19. Lan T, et al. (2007) Stabilized immune modulatory RNA compounds as agonists of Toll-like receptors 7 and 8. *Proc Natl Acad Sci USA* 104:13750–13755.
20. Scheel B, et al. (2006) Therapeutic anti-tumor immunity triggered by injections of immunostimulating single-stranded RNA. *Eur J Immunol* 36:2807–2816.
21. Eberle F, et al. (2008) Modificationsin small interfering RNA that separate immunostimulation from RNA interference. *J Immunol* 180:3229–3237.
22. Sioud M (2005) Induction of inflammatory cytokines and interferon responses by double-stranded and single-stranded siRNAs is sequence-dependent and requires endosomal localization. *J Mol Biol* 348:1079–1090.
23. Nguyen DN, et al. (2009) Drug delivery-mediated control of RNA immunostimulation. *Mol Ther* 17:1555–1562.
24. Robbins M, et al. (2008) Misinterpreting the therapeutic effects of small interfering RNA caused by immune stimulation. *Hum Gene Ther* 19:991–999.
25. Schroeder A, Levins CG, Cortez C, Langer R, Anderson DG (2010) Lipid-based nanotherapeutics for siRNA delivery. *J Intern Med* 267:9–21.
26. Whitehead KA, Langer R, Anderson DG (2009) Knocking down barriers: advances in siRNA delivery. *Nat Rev Drug Discov* 8:129–138.
27. Akinc A, et al. (2008) A combinatorial library of lipid-like materials for delivery of RNAi therapeutics. *Nat Biotechnol* 26:561–569.
28. Nguyen DN, et al. (2009) A novel high-throughput cell-based method for integrated quantification of type I interferons and in vitro screening of immunostimulatory RNA drug delivery. *Biotechnol Bioeng* 103:664–675.
29. Forsbach A, et al. (2008) Identification of RNA sequence motifs stimulating sequence-specific TLR8-dependent immune responses. *J Immunol* 180:3729–3738.
30. Semple SC, et al. (2010) Rational design of cationic lipids for siRNA delivery. *Nat Biotechnol* 28:172–176.
31. Barchet W, et al. (2005) Dendritic cells respond to influenza virus through TLR7- and PKR-independent pathways. *Eur J Immunol* 35:236–242.
32. Megjugorac NJ, Young HA, Amrute SB, Olshalsky SL, Fitzgerald-Bocarsly P (2004) Virally stimulated plasmacytoid dendritic cells produce chemokines and induce migration of T and NK cells. *J Leukoc Biol* 75:504–514.
33. Davila E, Celis E (2000) Repeated administration of cytosine-phosphorothiolated guanine-containing oligonucleotides together with peptide/protein immunization results in enhanced CTL responses with anti-tumor activity. *J Immunol* 165:539–547.
34. Halperin SA, et al. (2006) Comparison of the safety and immunogenicity of hepatitis B virus surface antigen co-administered with an immunostimulatory phosphorothioate oligonucleotide and a licensed hepatitis B vaccine in healthy young adults. *Vaccine* 24:20–26.
35. Vollmer J, Krieg AM (2009) Immunotherapeutic applications of CpG oligodeoxynucleotide TLR9 agonists. *Adv Drug Deliv Rev* 61:195–204.
36. Malyala P, O'Hagan DT, Singh M (2009) Enhancing the therapeutic efficacy of CpG oligonucleotides using biodegradable microparticles. *Adv Drug Deliv Rev* 61:218–225.
37. Wilson KD, de Jong SD, Tam YK (2009) Lipid-based delivery of CpG oligonucleotides enhances immunotherapeutic efficacy. *Adv Drug Deliv Rev* 61:233–242.
38. Cooper CL, Angel JB, Seguin I, Davis HL, Cameron DW (2008) CPG 7909 adjuvant plus hepatitis B virus vaccination in HIV-infected adults achieves long-term seroprotection for up to 5 years. *Clin Infect Dis* 46:1310–1314.
39. Schlee M, Hornung V, Hartmann G (2006) siRNA and isRNA: Two edges of one sword. *Mol Ther* 14:463–470.
40. Sioud M (2007) RNA interference and innate immunity. *Adv Drug Deliv Rev* 59:153–163.
41. Weinstein S, Peer D (2010) RNAi nanomedicines: Challenges and opportunities within the immune system. *Nanotechnology* 21:232001.
42. Putnam D (2006) Polymers for gene delivery across length scales. *Nat Mater* 5:439–451.
43. Love KT, et al. (2010) Lipid-like materials for low-dose, in vivo gene silencing. *Proc Natl Acad Sci USA* 107:1864–1869.
44. Mahon KP, et al. (2010) Combinatorial approach to determine functional group effects on lipidoid-mediated siRNA delivery. *Bioconjug Chem* 21:1448–1454.
45. Asselin-Paturel C, Brizard G, Pin J-J, Briere F, Trinchieri G (2003) Mouse strain differences in plasmacytoid dendritic cell frequency and function revealed by a novel monoclonal antibody. *J Immunol* 171:6466–6477.
46. Jurk M, et al. (2002) Human TLR7 or TLR8 independently confer responsiveness to the antiviral compound R-848. *Nat Immunol* 3:499–499.
47. Gorden KK, et al. (2006) Oligodeoxynucleotides differentially modulate activation of TLR7 and TLR8 by imidazoquinolines. *J Immunol* 177:8164–8170.
48. Martinez J, Huang X, Yang Y (2010) Toll-like receptor 8-mediated activation of murine plasmacytoid dendritic cells by vaccinia viral DNA. *Proc Natl Acad Sci USA* 107:6442–6447.
49. Horsmans Y, et al. (2005) Isatoribine, an agonist of TLR7, reduces plasma virus concentration in chronic hepatitis C infection. *Hepatology* 42:724–731.
50. Fidock MD, et al. (2011) The innate immune response, clinical outcomes,and ex vivo HCV antiviral efficacy of a TLR7 agonist (PF-4878691). *Clin Pharmacol Ther* 89:821–829.
51. Fletcher S, Steffy K, Averett D (2006) Masked oral prodrugs of toll-like receptor 7 agonists: A new approach for the treatment of infectious disease. *Curr Opin Investig Drugs* 7:702–708.
52. Savage P, et al. (1996) A phase I clinical trial of imiquimod, an oral interferon inducer, administered daily. *Br J Cancer* 74:1482–1486.
53. Seder RA, Darrah PA, Roederer M (2008) T-cell quality in memory and protection: Implications for vaccine design. *Nat Rev Immunol* 8:247–258.
54. Barr TA, Brown S, Mastroeni P, Gray D (2009) B cell intrinsic MyD88 signals drive IFN-gamma production from T cells and control switching to IgG2c. *J Immunol* 183:1005–1012.
55. Tritto E, Mosca F, De Gregorio E (2009) Mechanism of action of licensed vaccine adjuvants. *Vaccine* 27:3331–3334.
56. Chikh G, et al. (2009) Synthetic methylated CpG ODNs are potent in vivo adjuvants when delivered in liposomal nanoparticles. *Int Immunol* 21:757–767.

Supporting Information

Nguyen et al. 10.1073/pnas.1121423109

Material and Methods.

RNA. RNAs were fully phosphorothioate-modified, 20-base, single-stranded RNA synthesized by Coley Pharmaceuticals with sequences as previously described (1): R-006 [5′-UUGUUGUU-GUUGUUGUUGUU-3′] and R-1263 [5′-GCCACCGAGCC-GAAGGCACC-3′].

Combinatorial Lipidoid Synthesis. Lipidoids (2) were synthesized, as previously described, in a combinatorial fashion as depicted in Fig. S1*B* in solvent-free conditions by reacting primary and secondary amine-containing cores (Fig. S1*A*, *Right*) with alkyl-acrylate or alkyl-acrylamide (Fig. S1*A*, *Left*) tails at a high tail-to-core monomer ratio to drive synthesis of fully (n)-substituted lipidoids. Lipidoid products were purified of unreacted core and side-chain reactants resulting in crude mixtures of fully and incompletely substituted lipidoids by silica gel chromatography. Some alkyl-acrylate-tail lipidoids were further reacted with methyl iodide (MeI) (Fig. S1*C*) to form quaternized amines with a permanent positive charge.

Second-generation lipidoids were synthesized in a four-step process (Fig. S1*D*). The 100-core diamine was monoprotected by reacting 10x molar excess pure diamine with di-tert-butyl dicarbonate (Boc_2O). ND tails were reacted with the free primary amine in excess prior to deprotection and regeneration of the opposite primary amine resulting in ND(2)-100. ND(2)-100 was further reacted with NA or LD tails and purified into three-tail or four-tail derivatives, which have been renamed lipidoids I and II for clarification. Lipidoid nomenclature reflects alkyl tail linkage (acrylate $= L$, acrylamide $= N$), alkyl tail carbon-chain length ($A = 9$, $B = 10$, $D = 12$, $F = 14$, $G = 15$, $P = 16$, $H = 18$ carbons), and amine-containing core. Quaternized core-amines are renamed with a Q designation instead of L. Purified lipidoids include number of tails in parentheses following tail name. A complete list of crude lipidoids screened is found in Table S1.

High-Throughput Screening for Lipidoid-Mediated Immunostimulatory RNA (isRNA) Delivery. Donor-blind buffy-coat packs were obtained from the Massachusetts General Hospital blood bank. Peripheral blood mononuclear cells (PBMC) were isolated by Ficoll-Paque Plus (Amersham Biosciences) density centrifugation. PBMCs were resuspended in supplemented RPMI medium 1640 (RPMI medium 1640 with 10% FCS, 1 mM MEM sodium pyruvate, 10 mM Hepes, and 100 U/mL penicillin/streptomycin) and plated at 5×10^5 cells/well in 175 μL in 96-well tissue culture plates. Lipofectamine 2000 (L2K) (Invitrogen) was used as a positive control for transfection of RNA according to manufacturer's protocols and to normalize interferon responses across different donors.

Crude or purified lipidoid products were dissolved to 0.5 mg/mL in 25 mM sodium acetate (pH 5), followed by brief sonication. For lipidoids with poor solubility, up to 10% DMSO was added to stock lipidoid solutions. RNA was dissolved to 50 μg/mL in sodium acetate. Lipidoids were arrayed in 96-well round-bottom reaction plates and mixed at 15, 10, 5, and 2.5:1 mass ratios of lipid to RNA for 80 μL total volume. After 20 min incubation at room temperature to allow for nanoparticle complexes to form, complexes were diluted with 120 μL RPMI medium 1640. In quadruplicate, 25 μL of diluted complexes were added to PBMCs for a final RNA concentration of 200 ng RNA per well in 200 μL media (1 μg/mL approximately 140 nM). After 16–20 h of incubation, PBMC cultures were centrifuged at 400 × g relative centrifugal force (rcf) for 10 min, and supernatants were stored at −80 °C for later quantification.

Type I interferon activity was quantified using a high-throughput (HT)-compatible cell-based detection assay as previously described (3). Briefly, 293T-ISRE-RFP cells were incubated with 50 μL PBMC supernatant overnight prior to HT-FACS analysis of red fluorescence. Recombinant human interferon alpha (h IFN-α) (PBL Laboratories) serially diluted in supplemented RPMI medium 1640 was used as a standard, and type I interferon activity of each screening well was normalized to L2K-mediated transfection with R-006 to control for donor PBMC variability in maximum type I interferon secretion capacity.

Formulation and Characterization of Lipidoid-RNA Nanoparticles. Purified lipidoid was dissolved to 120 mg/mL in ethanol. Cholesterol (Ch) (Sigma Aldrich) was dissolved to 25 mg/mL in ethanol. N-palmitoyl-sphingosine-1-[succinyl(methoxypolyethylene glycol)2000] (C16 mPEG 2000 ceramide) (PEG) (Avanti Polar Lipids) was dissolved to 100 mg/mL in ethanol. Lipidoid, Ch, and PEG were combined at a 15:0.8:7 mass ratio (L:C:P), vortexed briefly, and diluted in a mixture of ethanol and 200 mM sodium acetate (with 16.67 mg/mL sucrose for lyophilization) for a final lipidoid concentration of 7.5 mg/mL in 35% ethanol, 65% sodium acetate. RNAs were resuspended in water to 10 mg/mL and diluted with 35% ethanol. Lipidoid/Ch/PEG were added to diluted RNA at a 15, 11.5, or 10:1 mass ratio (L:R) and vortexed for 20 min to allow complexes to form. Complexed lipidoid–RNA nanoparticles were extruded once through a double 200 nm membrane and then twice through a double 80 nm membrane (Whatman) on a Northern Lipids extrusion system at 40 °C. To remove ethanol prior to injection, nanoparticles were dialyzed in a Slide-A-Lyzer 3500 molecular weight cutoff dialysis cassette (Pierce Biotech) against HBSS. For lyophilization, 10 mg of sucrose was added per milliliter of extruded complexes prior to freezing at −80 °C for >2 h followed by >1 d lyophilization.

For quantification and encapsulation efficiency of RNA, a 50 μL sample of nanoparticles was diluted 200-fold in Tris-EDTA buffer (TE), mixed with either 50 μL of TE buffer or 50 μL of 2% Triton-X-100 (T-X) in TE, and incubated with 100 μL Quant-It Ribogreen reagent (Invitrogen) for 20 min at 37 °C in a 96-well black plate. Total fluorescence in the presence of T-X was compared to a standard curve of RNA diluted in TE to determine total RNA concentration; RNA encapsulation efficiency was determined by the ratio of fluorescence signal without T-X and with T-X. Nanoparticle size and zeta potential of formulated lipidoid–RNA nanoparticles was assayed by dynamic light scattering using a Zeta-PALS instrument (Brookhaven Instruments) after 1/50 dilution in PBS or with a Mastersizer instrument (Malvern Instruments) after dilution in HBSS. No bacterial endotoxin was detected by limulus amebocyte lysate assay (Lonza) in any batches of nanoparticles.

In Vitro Characterization of Innate Immune Responses. Human PBMCs were collected as described above and further purified into PDC ($BDCA2^+$) and monocyte ($CD14^+$) populations by positive selection with magnetic-assisted sorting according to manufacturer's protocols (Miltenyi Biotech). Cells were then incubated for 24 h with three-tail lipidoid-RNA nanoparticles formulated for in vitro transfection. Supernatants were analyzed for type I interferon activity by cell-based 293T-ISRE-RFP assay as described above.

A reporter plasmid expressing luciferase controlled by multiple Nf-κB-inducible promoter regions, pNifty-Luciferase (Invivogen), was transfected into HEK293T cell lines stably expressing indicated human TLRs (Invivogen). These cells were stimulated in vitro with lipidoid I-4 + isRNA nanoparticles at 4 μg/mL RNA for HEK293T cells expressing TLR2/6, TLR3, TLR4, TLR5, or TLR9; or at a range of RNA concentrations for HEK293T cells expressing TLR7 or TLR8. As positive controls, cells were also stimulated with known TLR-specific ligands: synthetic diacylated lipoprotein FSL-1 (TLR2/6), poly(I:C) (TLR3), lipopolysaccharide (LPS) (TLR4), flagellin (TLR5), garadiquimod (TLR7), CL097 (TLR8), CpG oligodeoxynucleotide 2395 (TLR9); all purchased from Invivogen and used at manufacturer's recommended concentrations. Luciferase activity was determined after 24 h using the Bright-Glo assay (Promega) according to manufacturer's protocols.

In Vivo Characterization of Innate Immune Responses. To further investigate RNA-specific immune responses, lipidoid–RNA nanoparticles were formulated with either R-006 or R-1263 at 15:1 ratio (lipidoid to RNA), dialyzed to remove ethanol, and diluted in HBSS prior to injection under isofluorane anesthesia. All animal studies, except for influenza prophylaxis studies, were conducted at Coley Pharmaceuticals (now Pfizer, Canada; Ottawa, ON, Canada) under the approval of the institutional care committees and in accordance with the guidelines set forth by the Canadian Council on Animal Care. Mouse studies of influenza prophylaxis were conducted at the Massachusetts Institute of Technology (Cambridge, MA). Male 129Sv mice were purchased from Taconic Farms and cared for according to the standards of the Massachusetts Institute of Technology under the guidance of the Division of Comparative Medicine. Animals were monitored for the duration of all experiments for adverse behaviors, which might indicate toxicity or adverse inflammatory responses, such as shivering, abnormal secretions, lethargy, decreased social interactions, or decrease in normal activity.

Formulated lipidoid–RNA nanoparticles, or blank nanoparticles without RNA at an equivalent total lipidoid dose, were diluted in HBSS prior to subcutaneous injection of 25 μg RNA in each flank under isofluorane anesthesia for a total dose of 50 μg RNA per mouse. After 9 h, mice were anesthetized with a mixture of ketamine (1 wt%) and xylazine (0.15 wt%) in PBS by i.p. injection. Mice were immediately infected by intranasal instillation with a supralethal dose of 12,000 plaque-forming units (pfu) of influenza A virus A/PR/8/34 (PR8) strain diluted in PBS with 0.3 wt% BSA and 100 U/mL penicillin/streptomycin. Mice were sacrificed 24 h after infection, whole lungs were flash frozen in 2 mL of PBS/BSA solution in liquid nitrogen, and lungs were subjected to two freeze-thaw cycles followed by sonication. Virus was extracted from lung homogenates after centrifugation at 800 × g rcf. Viral titer in harvested lungs was determined by plaque-forming assay. Madine–Darby canine kidney cells were seeded at 0.5×10^6 cells/well in six well plates in DMEM (with 10 mM Hepes, 10% FBS, 100 U/mL penicillin/streptomycin, 2 mM glucose) and allowed to grow to single-layer confluence overnight. Media was aspirated from wells, and 200 μL of virus-containing samples serially diluted 10-fold in PBS were added onto cells in triplicate. Following a 1 h incubation period with periodic shaking to distribute viral particles evenly, cells were covered with 2 mL of semisolid 1% agar/media solution to limit viral particle spread to cell-to-cell contacts. Plaques were counted after 3 d.

Innate immune responses of multiple lipidoid formulations with R-006 RNA were compared after s.c. injections at increasing doses in BALB/c mice or i.v. tail vein injection in 129Sv mice. TLR-mediated responses were investigated following i.v. injection in C57Bl/6, C57Bl/6 TLR7$^{-/-}$, C57Bl/6 TLR9$^{-/-}$, C57Bl/6 MyD88$^{-/-}$, C3H, or C3H TLR4$^{-/-}$. As a control, DOTAP [1,2-dioleoyloxy-3-(trimethylammonium)propane] (Roche) was complexed with RNA at a 2 : 1 weight ratio (L:R). Blood samples for serum isolation were taken by direct cardiac puncture on heparin at indicated timepoints. Serum samples were analyzed by ELISA with commercially available antibodies (IFN-α, PBL Labs) (IP-10, BD Pharmingen) or 10-plex Luminex technology (BioSource International). Splenocytes were also harvested for surface expression of activation markers by staining with anti-CD69-FITC, anti-CD86-APC, anti-CD3-PE/Cy7, anti-CD19-ECD, and anti-DX5-PE. Cytolytic activity of NK cells was measured by chromium release following in vitro incubation of splenocytes with YAC-1 target cells at indicated effector:target ratios.

Adjuvant studies of lipidoid–RNA nanoparticles were performed by mixing indicated doses of lipidoid-formulated RNA with 20 μg chicken ovalbumin (Ova) protein antigen immediately prior to i.m. injection into C57Bl/6 mice or MyD88$^{-/-}$ on the C57Bl/6 background. Mice were vaccinated with either Ova protein antigen alone, or Ova protein mixed with the TLR9 agonist CpG ODN 1826, the TLR3 agonist poly(I:C), or DOTAP-formulated RNA. Mice were dosed three times, at days 0, 14, and 21. After 28 d, blood was collected by direct cardiac puncture on heparin. Plasma antibody levels of anti-Ova total IgG, IgG1, and IgG2c were determined by sandwich ELISA. Splenocytes were also harvested at day 28 for flow cytometric analysis of surface expression markers and cytokine production. Splenocytes were directly stained for antigen-specific T-cells with anti-CD44-FITC, SIINFEKL-tetramer-PE, anti-CD8-ECD, anti-CD62L-APC, and anti-CD3-PE/Cy7. Separate aliquots of the same splenocyte samples were also independently stimulated in vitro with Ova protein in RPMI medium 1640 + 1% L-glutamine + 1% penicillin/streptomycin + 10% FBS + β-mercaptoethanol for 24 h. Supernatants were analyzed by ELISA after 24 h for IL-2, IL-4, IL-10, and TNFα, or after 72 h for IFN-γ.

1. Forsbach A, et al. (2008) Identification of RNA sequence motifs stimulating sequence-specific TLR8-dependent immune responses. *J Immunol* 180:3729–3738.
2. Akinc A, et al. (2008) A combinatorial library of lipid-like materials for delivery of RNAi therapeutics. *Nat Biotechnol* 26:561–569.
3. Nguyen DN, et al. (2009) A novel high-throughput cell-based method for integrated quantification of type I interferons and in vitro screening of immunostimulatory RNA drug delivery. *Biotechnol Bioeng* 103:664–675.

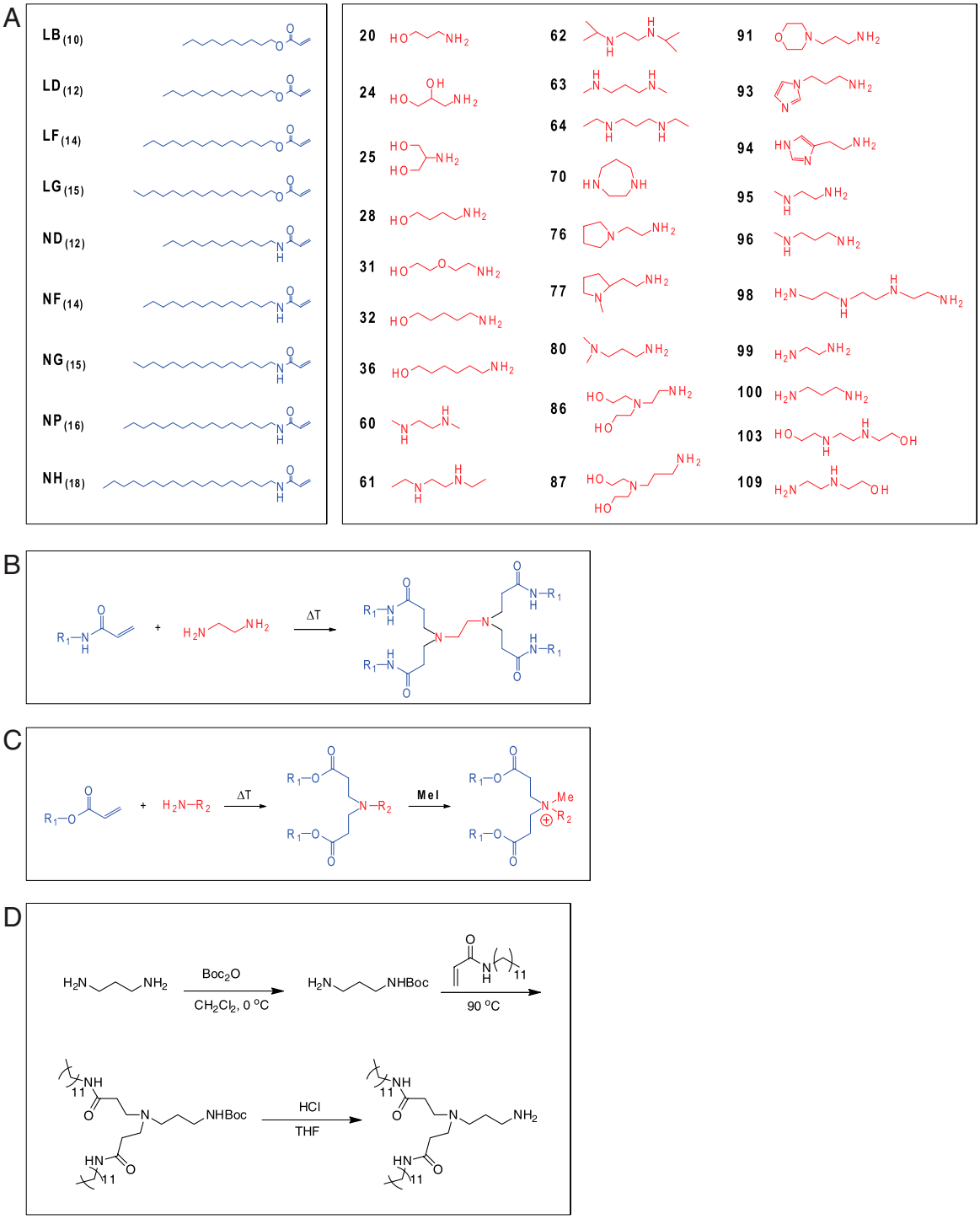

Fig. S1. (*A*) A subset of components from the larger lipidoid library (2) used in this study. When combined with amine-containing cores (red) to form lipid-like structures, alkyl-acrylate (L) tails form a hydrolysable ester bond, and alkyl-acrylamides (N) form nondegradable amine linkages. Tail groups (blue) are coded according to linkage and number of carbons in the alkyl chain. Lipidoid nomenclature reflects alkyl tail linkage (acrylate = L, acrylamide = N), alkyl tail carbon-chain length (A = 9, B = 10, D = 12, F = 14, G = 15, P = 16, H = 18 carbons), and amine-containing core (number). (*B*) Schematic of solvent-free batch synthesis process resulting in crude mixtures of lipidoid components. All reactions were performed in excess of tail groups to drive towards full substitution of all core amine groups. Primary amines may accept up to two tail substitutions and secondary amines can accept up to one. Crude products typically contain a mixture of fully n-substituted and n-1 substituted lipidoids with rare n-2 substitutions. (*C*) Lipidoids can be further reacted with methyl iodide (MeI) to form quaternary amines carrying a permanent positive charge. Quaternized lipidoids are renamed with a Q designation (Q lipidoids). (*D*) Synthesis of second-generation lipidoids (lipidoids I and II) based on the 100-core. Intermediate protection and deprotection steps were used to generate the ND(2)-100 precursor, which was further reacted with the NA or LD tails in the synthesis of mixed-tail lipidoids of the 100 core.

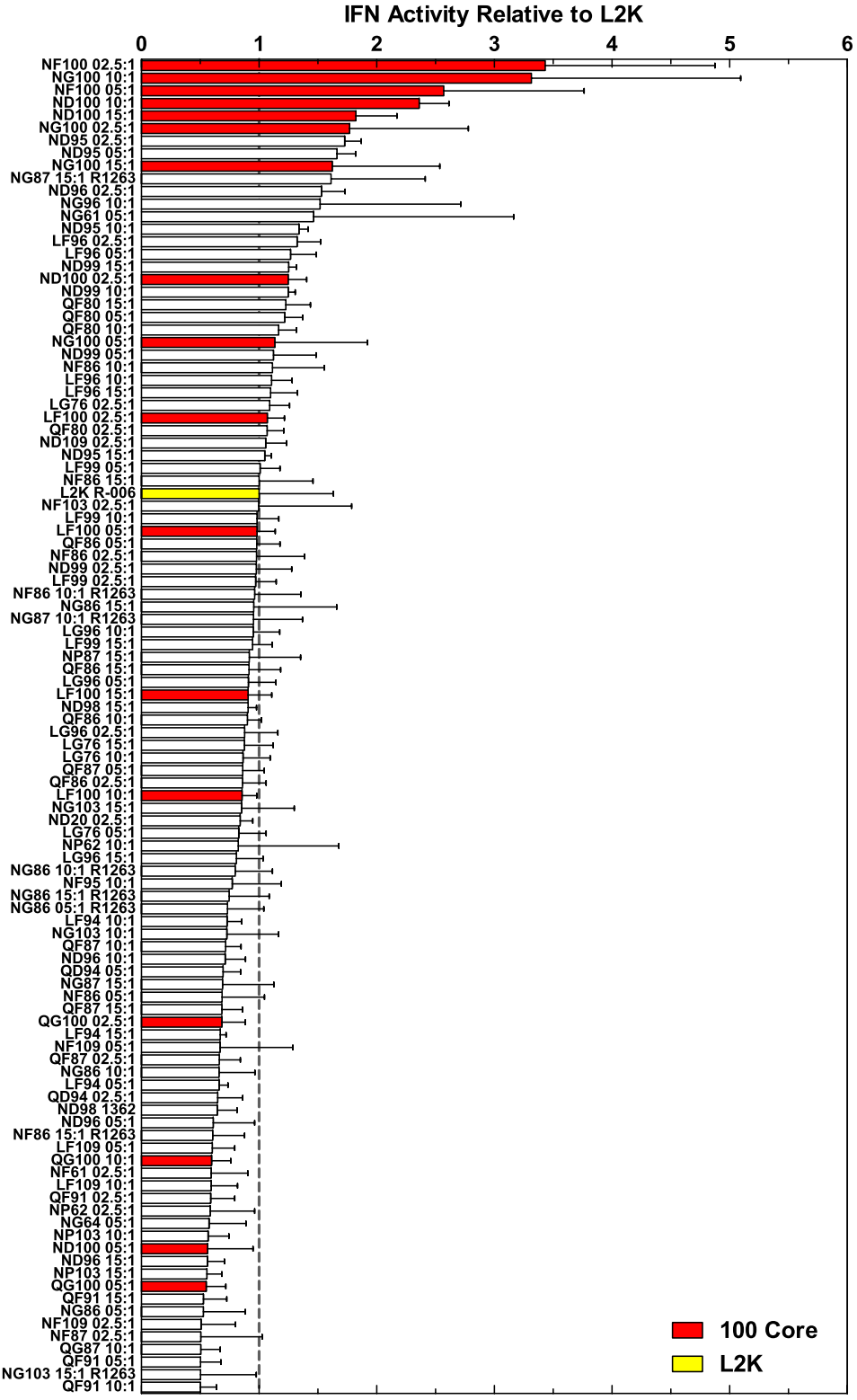

Fig. S2. Activity of all formulations (different lipidid, L:R ratio, or RNA) with relative in vitro immunostimulatory activity above 50% of the activity achieved with L2K. All 96 lipidoid compounds were screened for isRNA delivery in vitro at four different mass ratios of lipidoid to RNA (15, 10, 5, 2.5 to 1), with an immunostimulatory RNA (R-006) and control RNA (R-1263) comprising over 900 unique transfection experiments. Complexes were added to 5×10^5 human PBMCs in 96 well plates at 200 ng RNA per well (1 μg/mL approximately 140 nM) for 16–20 h. Type I interferon activity was determined by cell-based 293T-ISRE-RFP assay and activity was normalized for each batch of PBMCs to activity of L2K complexed with R-006 (dashed line = relative activity of 1). Unless noted, formulations are with the R-006 RNA. Lipidoids with the 100 core are colored in red. Each bar is the average of four repeats with standard deviation shown.

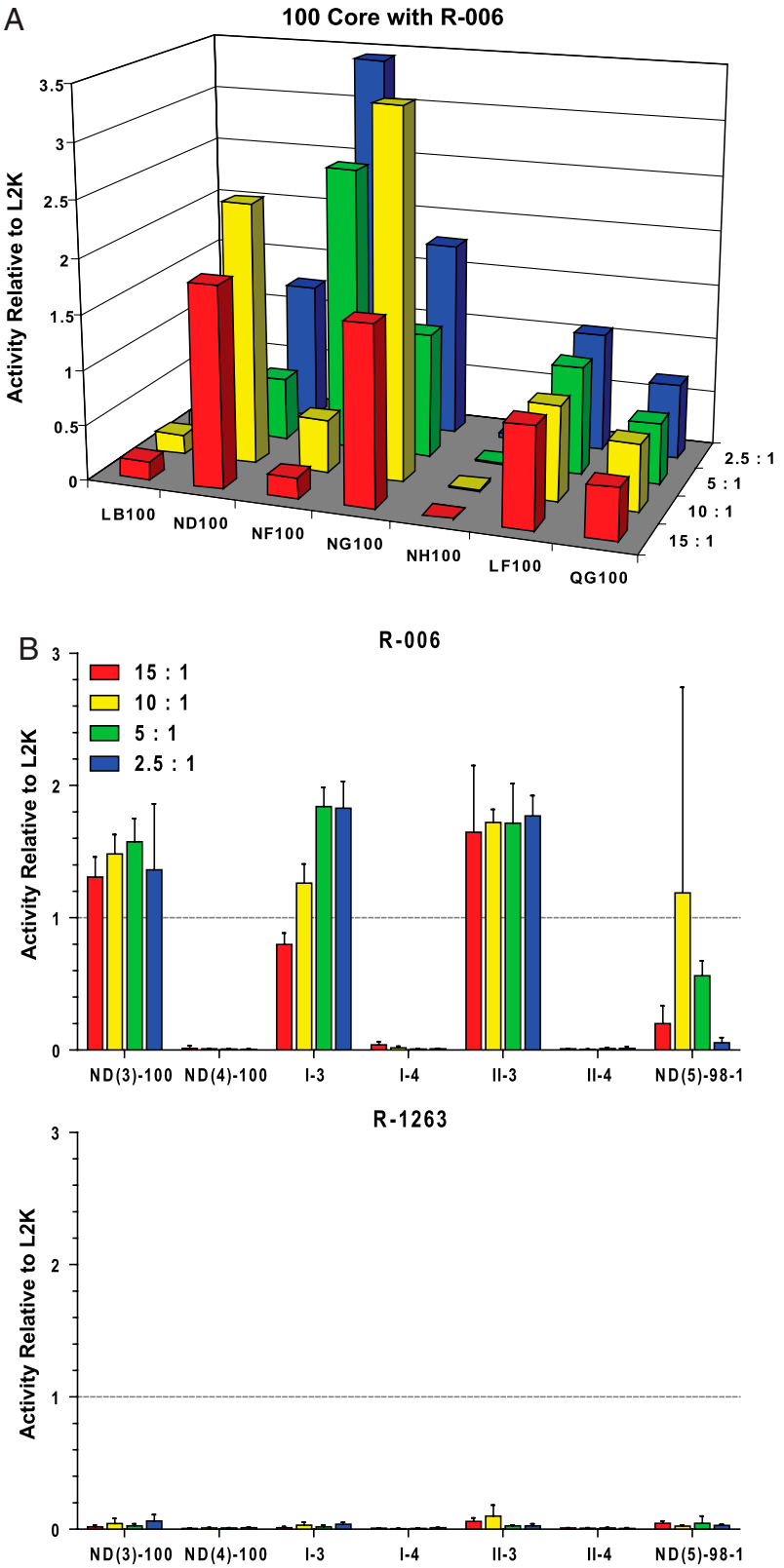

Fig. S3. Screening highlights immunostimulatory RNA delivery in vitro with 100-core lipidoids. (*A*) Type I interferon activity following human PBMC transfection with 100 core shown for all four weight ratios of lipidoid to RNA using immunostimulatory RNA R-006. Type I interferon activity was normalized to L2K delivery of R-006. Activity in vitro of all 100-core materials complexed with control RNA R-1263 was near or below detection limits. Lipidoid NH100 was insoluble in sodium acetate even after heating and sonication. Whereas NF100 had the highest activity of all lipidoids, the degradable version, LF100, was not as active. Further, quaternization of the degradable version of NG100 severely reduced delivery potential. (*B*) Structures and in vitro isRNA delivery characterization of second-generation lipidoids. Purified first- and second-generation lipidoids based on 100 core were screened in vitro for R-006 isRNA delivery with R-1263 RNA as a control. Fully substituted lipidoids (i.e., 100-core with four tails) were poorly soluble in sodium acetate. Type I interferon activity is normalized to transfection of R-006 with L2K (dotted line).

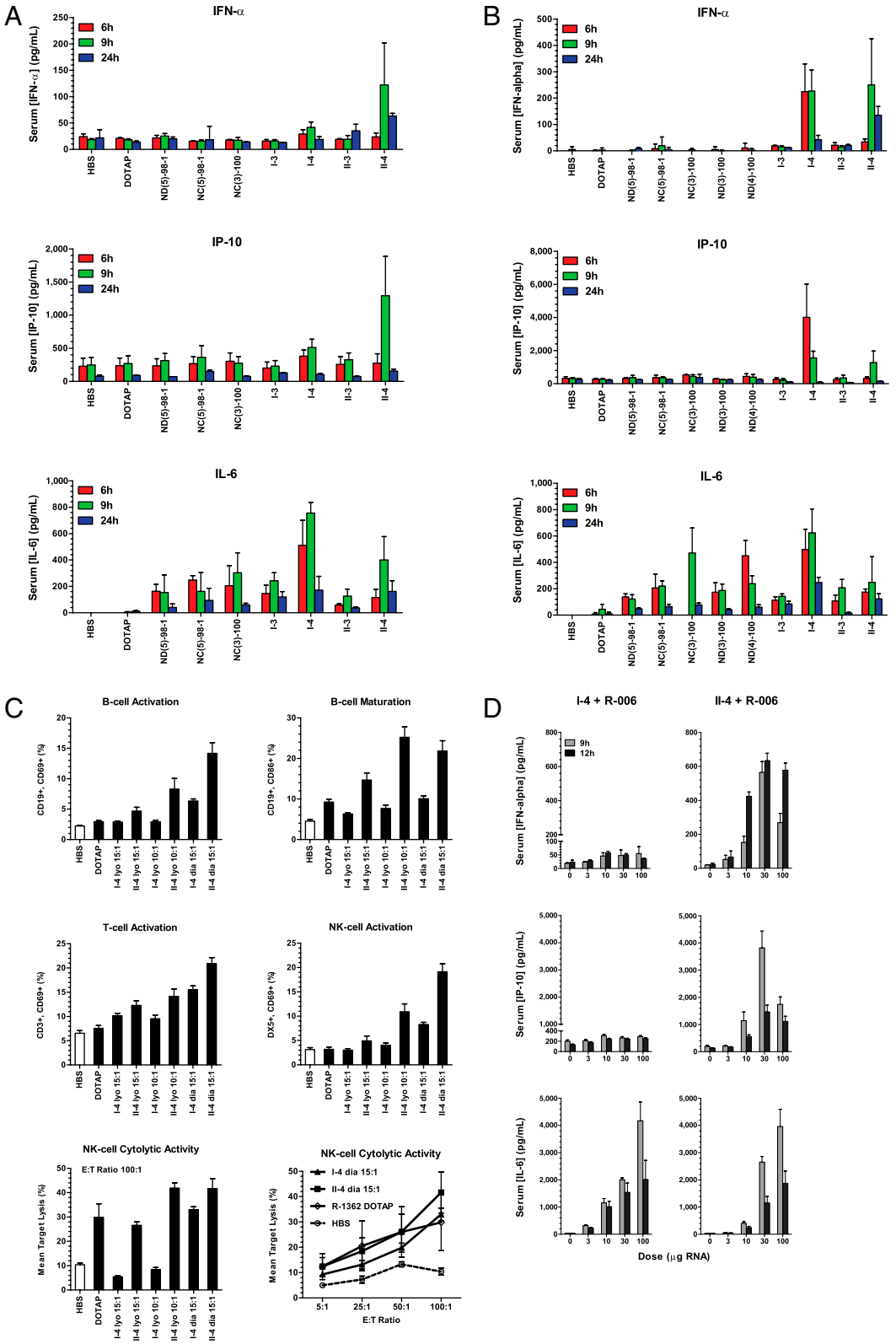

Fig. S4. In vivo screening for activation of innate immune responses following injection of formulated lipidoid–RNA nanoparticles. Lipidoid–RNA nanoparticles formulated with 100 ug R-006 RNA were injected s.c. in BALB/*c* mice ($n = 3$ or 4). R-006 formulated with DOTAP and a mock injection with HBSS were included as controls. (*A*) First round screening with lyophilized nanoparticles resuspended in HBSS. (*B*) Second round screening with nanoparticles dialyzed against HBSS for 2 h. (*A*–*B*) Blood was collected at 6, 9, 12, and 24 h following injection. Serum interferon-alpha, IP-10, and IL-6 cytokine levels were measured. (*c*) Comparison of lyophilized and dialyzed nanoparticles at either 10 : 1 or 15 : 1 wt : wt ratio of lipidoid:RNA. Spleens were also collected at 24 h for staining and FACS analysis of $CD3^+$ T-cell activation, $CD19^+$ B-cell activation and maturation, and $DX5^+$ NK-cell activation. Cytolytic activity of NK cells was measured by chromium release following in vitro incubation of splenocytes with YAC-1 target cells at indicated effector:target ratios. (*D*) Lipidoids I-4 [ND(2)NA(2)-100] and

II-4 [ND(2)LD(2)-100] were formulated with the strong TLR7/8 agonist R-006 RNA as well as the weak TLR7/8 agonist R-1263 RNA as control in liquid form. Dose–response of IFN-α (*Top*), IP-10 (*Middle*), and IL-6 (*Bottom*) at 9 and 12 h following s.c. injection into 129sv mice ($n = 4$) at 3, 10, 30, and 100 μg of nanoparticle-encapsulated R-006 RNA in lipidoid I-4 (*Left*) or II-4 (*Right*, note scale change for IFN-α and IP-10).

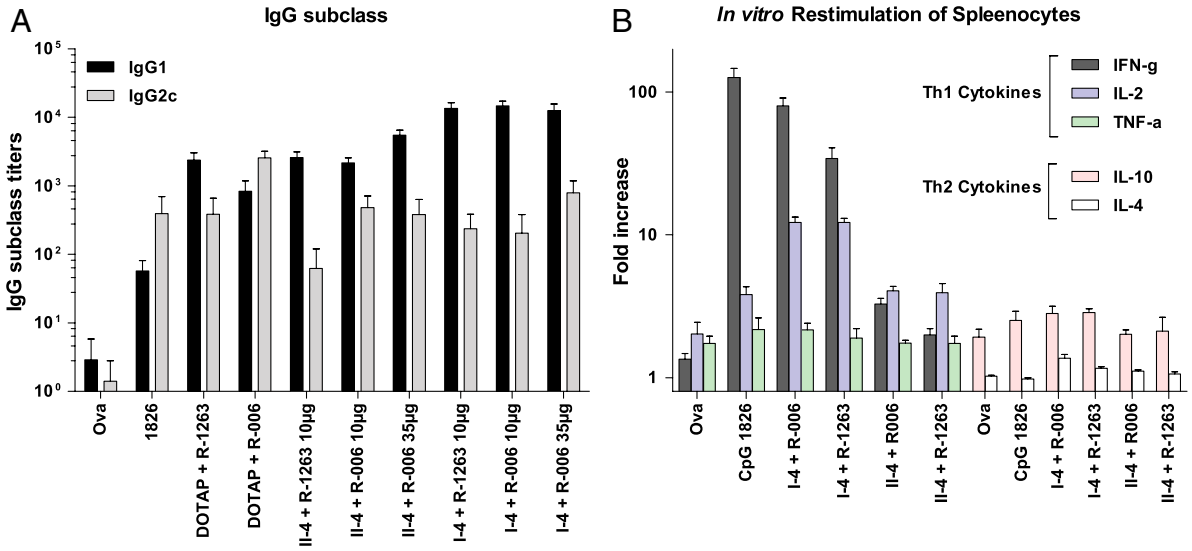

Fig. S5. Adjuvant activity in protein vaccination. Chicken ovalbumin protein vaccination in C57Bl/6 mice together with lipidoid I-4 or lipidoid II-4 nanoparticles formulated with R-006 RNA or R-1263 RNA at indicated doses. Mice were also vaccinated with Ova protein and DOTAP formulated RNA, unmethylated CpG ODN 1826, or without adjuvant. Immunization was performed intramuscularly on days 0, 14, and 21, and samples were collected at day 28. (*A*) Serum titers of Ova-specific IgG subclasses. (*B*) Relative increase in cytokine secretion following restimulation in vitro with Ova protein antigen for 24 h compared to un-stimulated.

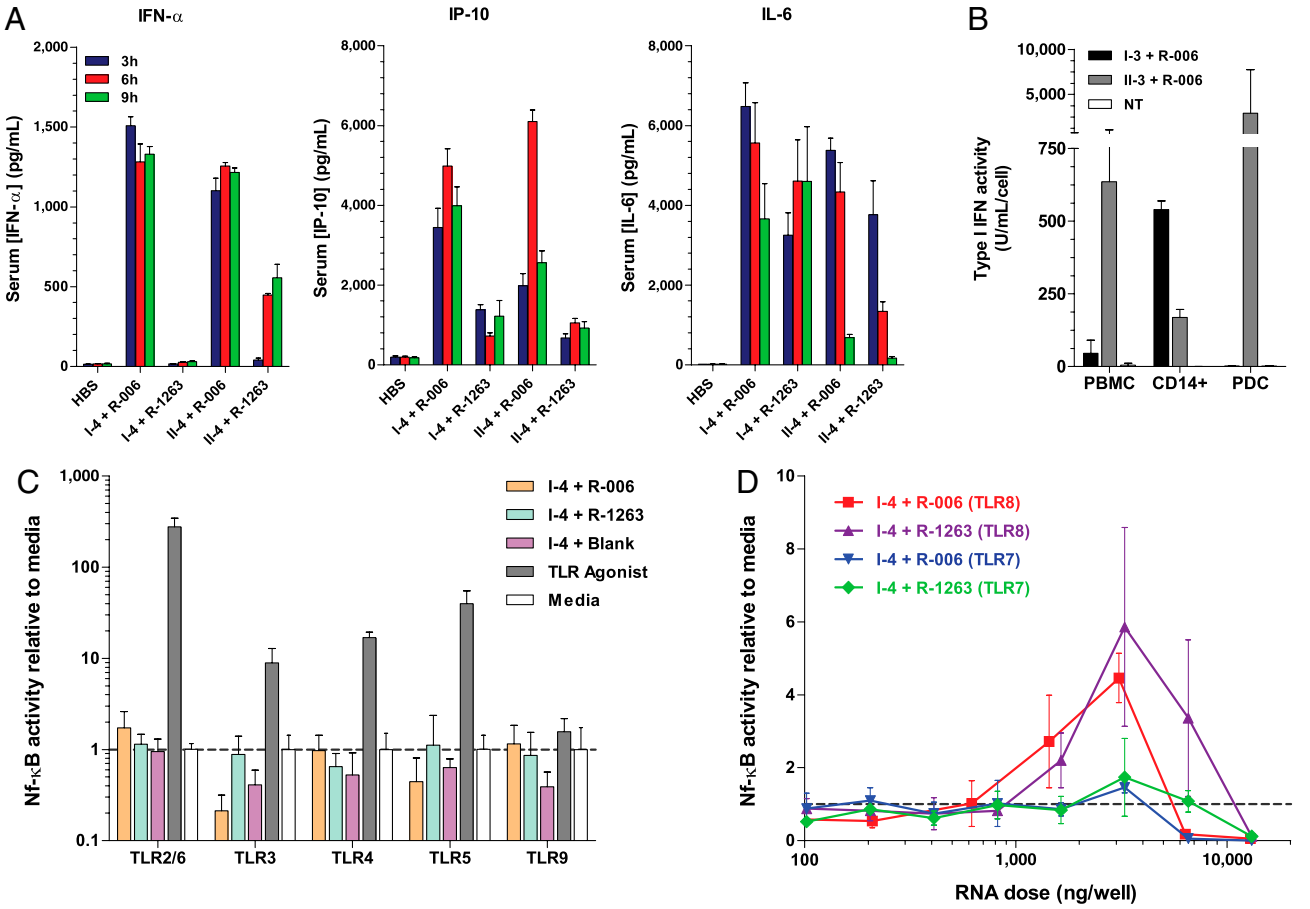

Fig. S6. (*A*) Lipidoids I-4 and II-4 were formulated with the strong TLR7/8 agonist R-006 RNA and the weak TLR7/8 agonist R-1263 RNA as control in dialyzed form. Serum cytokine responses of IFN-α (*Left*), IP-10 (*Center*), and IL-6 (*Right*) following i.v. injection into 129sv mice ($n = 4$) of 75 μg of active R-006 RNA or control R-1263 RNA formulated in lipidoid nanoparticles at 3, 6, and 9 h after injection. (*B*) Human PBMCs purified into PDC (BDCA2$^+$) and monocyte (CD14$^+$) populations were incubated for 24 h with nanoparticles of R-006 RNA and lipidoids I-3 [ND(2)NA(1)-100] or II-3 [ND(2)LD(1)-100], which are the three-tail versions of lipidoids I-4 and II-4, respectively. Supernatants were analyzed for type I interferon activity by cell-based 293T-ISRE-RFP assay, and activity is expressed in U/mL normalized to the total number of cells/well. (*C*–*D*) Nf-kB activity measured by luciferase reporter assay after stimulation of HEK293T cell lines stably expressing indicated human TLRs. Luciferase activity was determined after 24 h; data are expressed normalized to nonstimulated control wells filled with media only and indicated by the dashed line. (*C*) Stimulation of indicated TLR-expressing cell lines with lipidoid–RNA nanoparticles at 4 μg/mL RNA. (*D*) A range of lipidoid–RNA nanoparticle concentrations (expressed as an amount per well RNA basis) were used to stimulate HEK293T cells expressing TLR7 or TLR8.

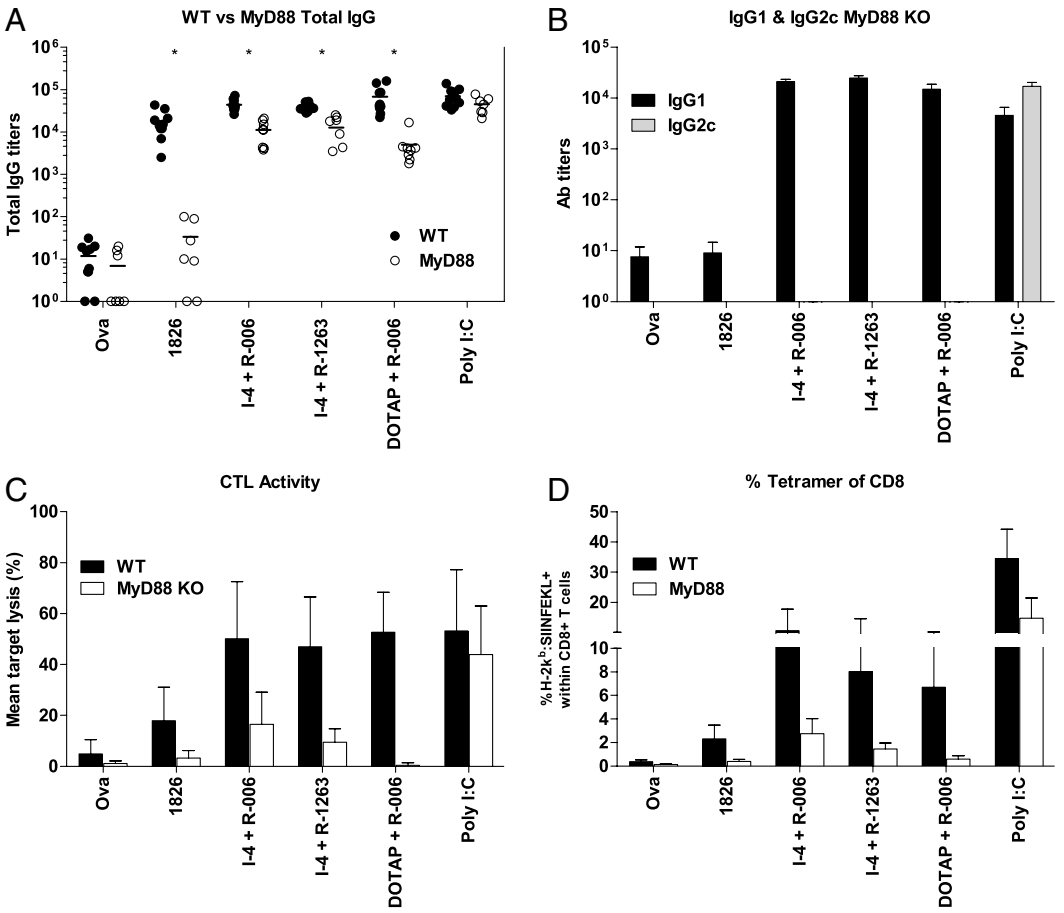

Fig. S7. Lipidoid I-4 nanoparticle adjuvant dependence on MyD88 following i.m. injection of 20 μg Ova protein with 35 μg RNA, CpG ODN 1826, or poly(I:C) RNA analogue at days 0, 14, and 21. (*A*) Total serum Ova-specific IgG titers in both WT and MyD88$^{-/-}$ mice, measured 28 d after first injection. (*B*) Serum titers in MyD88$^{-/-}$ mice of specific IgG1 and IgG2c classes measured 28 d after first injection. (*C*) Cytotoxic T lymphocyte (CTL) activity of both WT and MyD88$^{-/-}$ splenocytes after 5 d of restimulation with Ova antigen in vitro as measured by lysis of target cells at a 50:1 CTL:target ratio. (*D*) Total SIINFEKL-specific CD8^{+} T cells of both WT and MyD88$^{-/-}$ splenocytes after 5 d of restimulation with Ova antigen in vitro as measured by tetramer staining and flow cytometry. Poly(I:C) is a TLR3 ligand that acts independently of MyD88.

Table S1. List of the 96 crude lipidoid products screened

$ND_{(12)}$	$NF_{(14)}$	$NG_{(15)}$	$NP_{(16)}$	$NH_{(18)}$	L	Q
ND20	NF20	NG20	NP62	NH20	LB100	QD94
ND24	NF25	NG28	NP63	NH28	LB109	QD99
ND25	NF28	NG32	NP86	NH32	LD31	QD109
ND28	NF32	NG61	NP87	NH61	LD87	QF80
ND32	NF60	NG64	NP95	NH95	LF31	QF86
ND36	NF61	NG77	NP96	NH96	LF93	QF87
ND61	NF63	NG86	NP98	NH98	LF94	QF91
ND66	NF64	NG87	NP99	NH99	LF95	QG87
ND94	NF70	NG95	NP103	NH100	LF96	QG100
ND95	NF86	NG96	NP109	NH103	LF99	
ND96	NF87	NG98		NH109	LF100	
ND98	NF91	NG99			LF103	
ND99	NF95	NG100			LF109	
ND100	NF96	NG103			LG31	
ND109	NF98	NG109			LG76	
	NF99				LG96	
	NF100				LG93	
	NF103					
	NF109					

Lipidoids are organized by tail length and type as indicated. Alkyl-acrylamide tails ranged from ND (12 carbons) to NH (18 carbons). The alkyl-acrylate tails ranged from LB (10 carbons) to LG (15 carbons). A subset of lipidoids incorporating alkyl-acrylate tails were also quarternized (Q) to hold a static positive charge.

Table S2. Representative characteristics of lipidoid–RNA nanoparticles formulated in liquid form at 11.5:1 ratio after dialysis

Lipidoid	Effective diameter (nm)	Half width (nm)	Polydispersity	RNA encapsulation
ND(5)-98-1	71.4	28.8	0.163	88.3%
NC(5)-98-1	106.1	48.4	0.208	90.3%
NC(3)-116	83.1	33.8	0.165	91.6%
NC(3)-100	174.3	85.1	0.238	89.0%
I-3	112.4	53.6	0.227	91.9%
I-4	188.4	96.1	0.26	90.4%
II-3	142.8	54.5	0.145	90.9%
II-4	289.9	149.7	0.267	79.1%

Particle sizes were measured by dynamic light scattering. RNA encapsulation was determined by competitive binding of Ribogreen with Triton X-100.

Table S3. Representative characteristics of lipidoid–RNA nanoparticles

Lipidoid	Lipidoid:RNA ratio	Formulation	Peak 1 (nm)	Peak 2 (nm)	Polydispersity
ND(5)-98-1	15:1	lyophilized		2768	0.400
NC(5)-98-1	15:1	lyophilized	165	1507	0.900
NC(3)-100	15:1	lyophilized	264		0.400
ND(3)-100	15:1	lyophilized	146	707	0.756
ND(4)-100	15:1	lyophilized	87	659	1.000
I-4	15:1	lyophilized	83	560	1.000
II-4	15:1	lyophilized	144	1160	0.798
I-4	10:1	lyophilized		2946	1.000
II-4	10:1	lyophilized	73	1209	0.620
I-4	15:1	liquid	69		0.238
II-4	15:1	liquid	143		0.400

Lipidoid nanoparticles were formulated at 15:1 or 10:1 ratios and either dialyzed or resuspended after lyophilization for in vivo injection. Particle sizes were measured by dynamic light scattering, and the size (s) at peak intensity are indicated.